The Atmospheric Response to Sea Ice and Snow Cover Changes Induced by Global Warming

Michael Alexander (NOAA/ESRL; Boulder, CO; Michael.Alexander@noaa.gov) and Clara Deser, Robert Tomas, David Lawrence (NCAR, Boulder, CO)

Introduction

Northern Hemisphere sea ice and snow cover have decreased over the past several decades (Serreze et al. 2007; Déry and Brown, 2007) and these trends are projected to continue by climate models (Singarayer et al 2006; Seierstad and Bader 2009) as a result of global warming. For example, CCSM3, NCAR's coupled climate model indicates that sea ice will disappear during summer by the end of 21st century. However, snow and ice do not simply respond to the anthropogenic forcing but feedback on the climate system influencing the overall atmospheric response. This feedback of sea ice and terrestrial snow on climate is difficult to separate out from the radiative forcing and other effects in fully coupled models so here we use atmosphere only model experiments to examine their role in climate change. See Deser et al. 2010; Alexander et al. 2011.

Model Experiments

Three 60-year model simulations are conducted with the NCAR Community Atmosphere Model (CAM3) T85 resolution (~1.4° lat/lon) coupled to the Community Land Model (CLM3)

Control – sea ice and terrestrial snow prescribed to their 1980-1999 average obtained from CCSM3 simulations that include ocean and sea ice models in addition to CAM3 and CLM3.

Sea Ice – sea ice concentration and thickness prescribed to their 2080-99 average; snow cover set to 1980-99 mean value

Snow – fraction, depth and water content prescribed to their 2080-2099 average, sea ice set to 1980-99 mean value.

Experiment Design

1880-1999 values obtained from the average of the 7-member ensemble CCSM3 "20th century" simulations.

2080-2099 values obtained from the average of the 21st century CCSM3 simulations under the A1B greenhouse gas forcing scenario.

Boundary conditions repeat the same seasonal cycle in each experiment (no interannual variability).

SST and greenhouse gas concentrations set to the 1980-1999 CCSM3 output in all three experiments.

Response is obtained from the difference (Δ) between the 60-year average of the Sea ice or Snow (2080-99) with the control integrations (1980-99).

Statistical significance of the response evaluated using a two-sided t-test.

Sea Ice Experiments

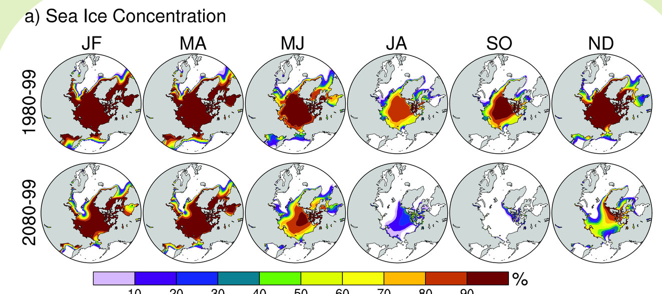

Bimonthly distributions of Arctic sea ice concentration (%) during 1980–99 and 2080–99 from CCSM3.

Sea Ice Forcing and Surface Flux response

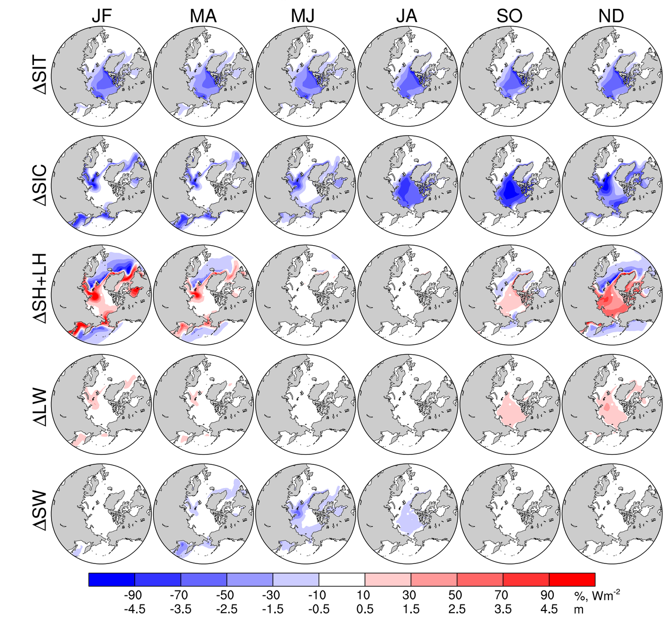

(Top two rows) Bi-monthly differences (2080-2099 minus 1980-1999 = Δ) Arctic sea ice thickness (ΔSIT; m) and concentration (ΔSIC; %) from CCSM3. (Bottom 3 rows) Bi-monthly turbulent energy flux (ΔSH+LH), longwave radiative flux (ΔLW) and shortwave radiative flux (ΔSW) responses to sea ice cover changes. Fluxes are given in units of Wm^{-2} and are positive upward.

Arctic Surface Energy Flux Response (Δ)

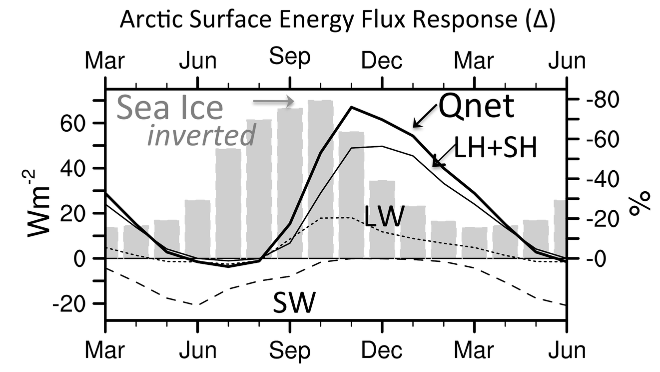

Seasonal cycle of the turbulent energy flux (Wm^{-2}; ΔSH + LH; thin solid curve), longwave radiative flux (÷ΔLW; dotted curve), and shortwave radiative flux (ΔSW; dashed curve) responses area averaged over the Arctic Ocean. The net surface energy flux response is given by the thick solid curve, and the SIC changes (%) are indicated by the gray bars (note the inverted scale). Fluxes are positive upward.

Net Surface Energy Flux & Air Temperature, Snow Depth and Precipitation Response

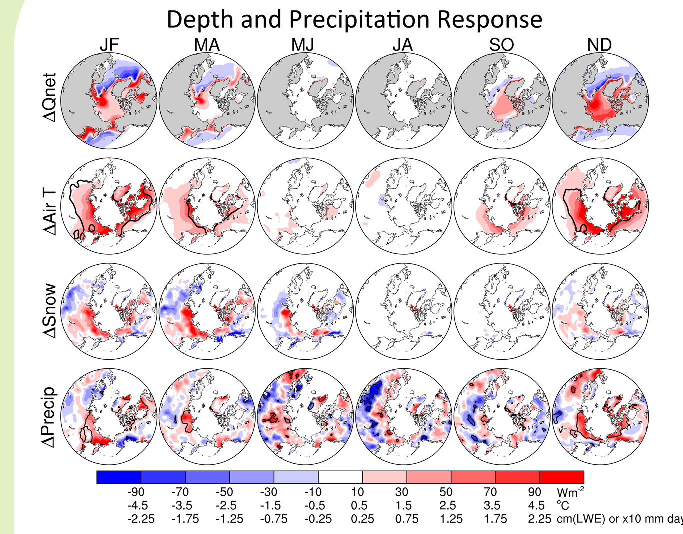

Bi-monthly response of net surface energy flux (ΔQnet; Wm^{-2}), terrestrial air temperature (ΔAir T; ºC), terrestrial snow depth (ΔSnow; cm liquid water equivalent) and terrestrial precipitation (ΔPrecip; mm day^{-1}). Thick black contours on the air temperature panels outline regions with a low-level temperature inversion ($T_{850hPa} - T_{1000hPa} > 0$ ºC) during 1980-1999. Precipitation responses significant at the 95% confidence level are outlined with black contours.

Vertical Structure of Air temperature December

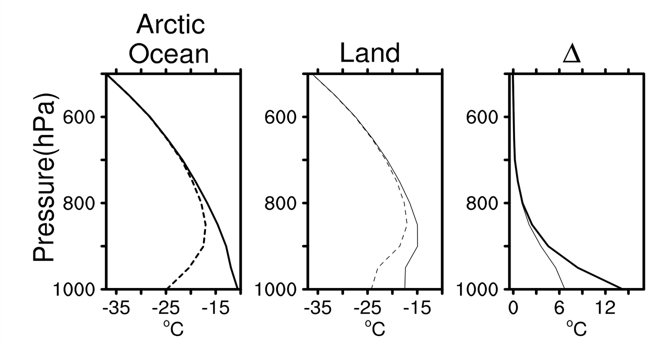

Vertical profiles of atmospheric temperature during 1980–99 (dashed curves) and 2080–99 (solid curves) over (left) the Arctic Ocean and (center) the high-latitude (65°–80°N) continents in December. (right) The 2080–99 minus 1980–99 differences over the Arctic Ocean (thick curve) and high-latitude continents (thin curve).

Geopotential Height Response (m)

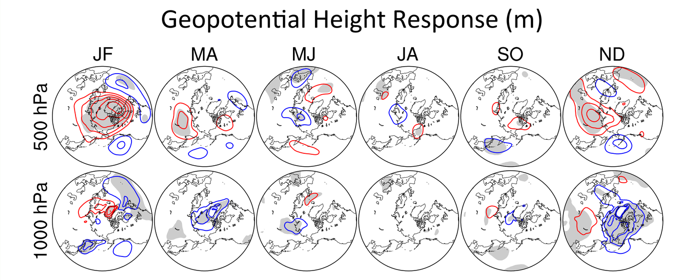

The geopotential height response (Δ*z*). The contour interval is 10 m, with positive (negative) values in red (blue) and the zero contours omitted. Shading indicates values that exceed the 5% confidence level based on a two-sided Student's *t* test.

Response to change in Sea Ice

- The loss of Arctic sea ice is greatest in summer and fall, yet the response of the net surface energy budget over the Arctic Ocean is largest in winter.
- Air temperature and precipitation responses also maximize in winter, both over the Arctic Ocean and over the adjacent high latitude continents.
- Snow depths increase over Siberia and northern Canada due to the enhanced winter precipitation and temperatures that remain below freezing.
- Atmospheric warming over the high latitude continents is mainly confined to the boundary layer (below ~ 850 hPa) and to regions with a strong low-level temperature inversion.
- Enhanced warm air advection by sub-monthly transient motions is the primary mechanism for the terrestrial warming (Deser et al. 2010).
- Significant large-scale atmospheric circulation response is found during winter, with a baroclinic vertical structure over the Arctic in November-December and a barotropic response in January-March. Response resembles the negative phase of the North Atlantic Oscillation in February only.
- Comparison with the fully coupled model reveals that Arctic sea ice loss accounts for most of the high latitude warming response to greenhouse gas forcing at the end of the 21st century.

Snow Experiments

Seasonal Snow Cover and Snow Depth

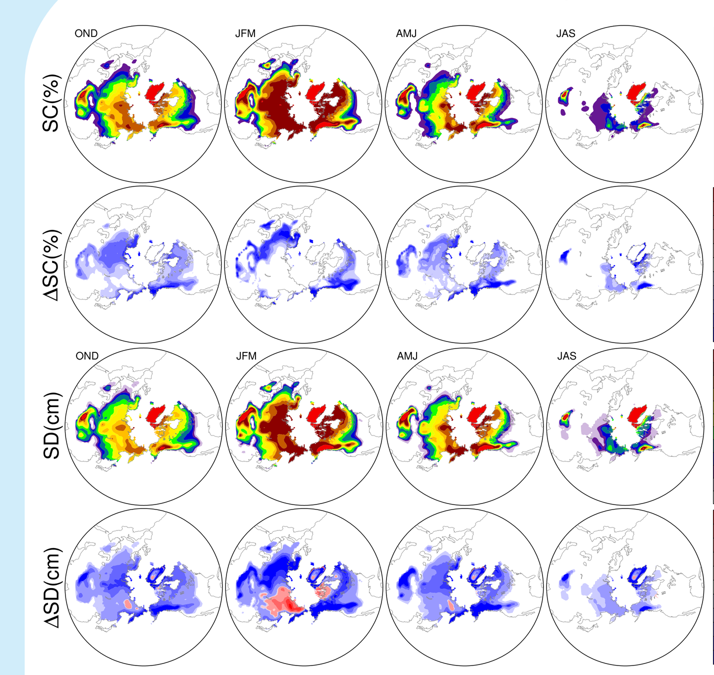

Seasonal distributions of the average terrestrial snow cover (SC, %) for (first row) 1980–99 and (second row) 2080–99 – 1980–99 (Δ) and (third and fourth rows) the same distributions for Snow depth (SD, cm) obtained from the CCSM3 and used as boundary conditions for the Snow experiments

Geopotential Height Response (m)

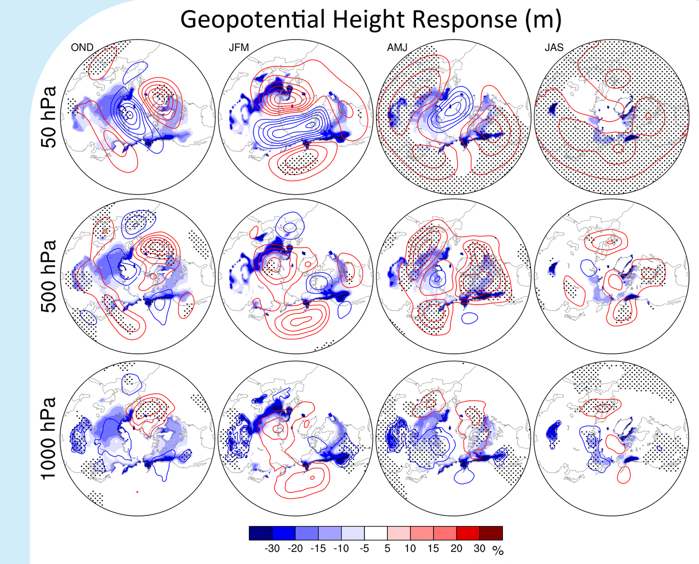

The geopotential height response (Δ*z*). The contour interval is 5 m with positive (negative) values in red (blue), and the zero contour is omitted. Stippling indicates values that exceed the 95% confidence interval; color shading denotes ΔSC (%).

Vertical profiles of ΔTemperature (°C)

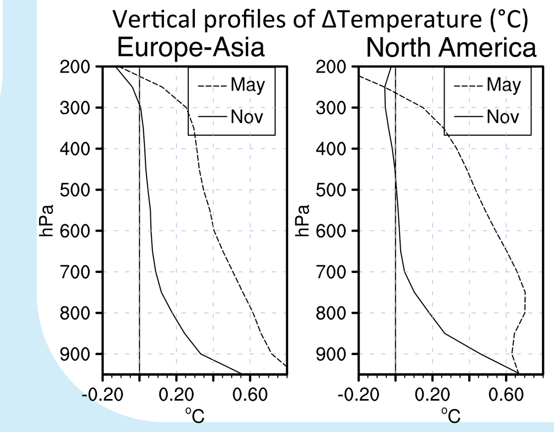

Vertical profiles of Δ*T* (°C) during November (solid line) and May (dashed line) over Eurasia and North America.

Response to Change in Snow Cover

- The reduction in snow cover increases the solar radiation absorbed by the surface, enhances upward longwave radiation, latent and sensible fluxes (Alexander et al. 2011)
- Surface air temperature changes are relatively small (< 3°C) compared with those due to Arctic sea ice changes (~10°C).
- However, they are continental in scale and are largest in fall and spring when they make a significant contribution to the overall warming over Eurasia and North America in the 21st century.
- The circulation response, while of modest amplitude, appears to involve multiple components including: remote Rossby wavetrains; an annular pattern that is strongest in the stratosphere; and a hemispheric increase in geopotential height.

Temperature Response Snow & Ice Experiments

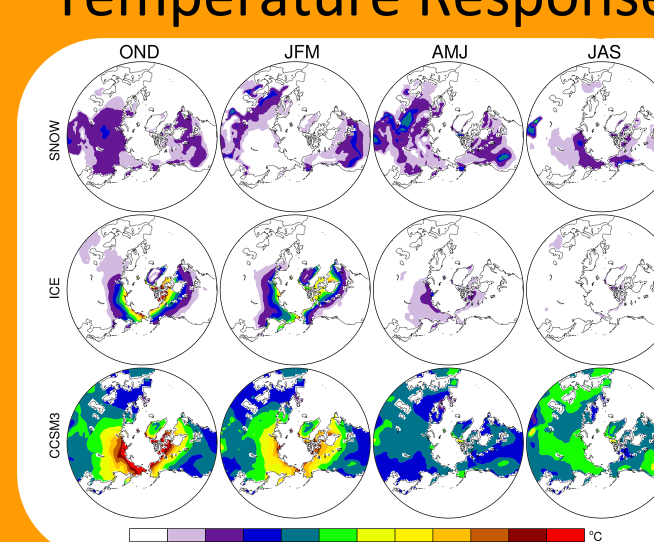

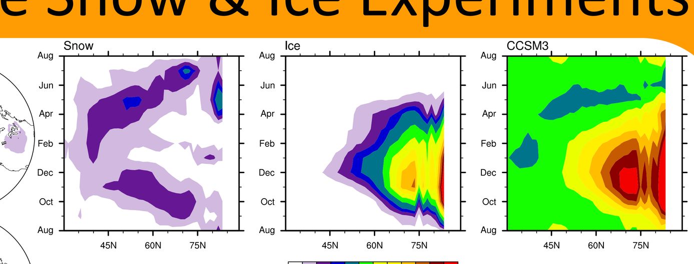

(Left): The ΔSAT (°C) over land in the (top): Snow, (middle): Sea Ice, and (bottom): original CCSM3 simulations (see Deser et al. 2010). All of the ΔSAT values >1.0°C and most values >0.5°C are statistically significant at the 95% level. (Above): Hovmöller diagrams of ΔSAT averaged over land as a function of latitude and calendar month in the (left): Snow, (middle): Sea Ice, and (right): CCSM3 experiments.

References

Alexander, M. A., R. Tomas, C. Deser, and D. M. Lawrence, 2010: The Atmospheric Response to Projected Terrestrial Snow Changes in the Late 21st Century *J. Climate*, **23**, 6430-6437.

Déry ,S. J., and R. D. Brown (2007), Recent Northern Hemisphere snow cover extent trends and implications for the snow-albedo feedback, Geophys. Res. Lett., 34, L22504, doi:10.1029/2007GL031474.

Deser, C., R. Thomas, M. Alexander, and D. Lawrence, 2010: The Seasonal Atmospheric Response to Projected Arctic Sea Ice Loss In the Late 21st Century. *J. Climate*, 23, 333-351.

Seierstad, I. A., and J. Bader, 2008: Impact of a projected future Arctic sea ice reduction on extratropical storminess and the NAO, *Clim. Dyn*. doi10.1007/s00382-008-0463-x.

Serreze, M. C., M. M. Holland, and J. Stroeve, 2007: Perspectives on the Arctic's shrinking sea-ice cover. *Science*, 315, 1533-1536.

Singarayer, J. S., J. L. Bamber and P.J. Valdes, 2006: Twenty-first-Century climate impacts from a declining Arctic sea ice cover. J. Climate, 19, 1109-1125.

This research was supported by a grant from the National Science Foundation's Arctic System Science Program